Orbital distortion and electric field control of sliding ferroelectricity in a boron nitride bilayer

Orbital distortion and electric field control of sliding ferroelectricity in a boron nitride bilayer

Meng Liu,[1] Hongyan Ji,[1] Zhaoming Fu,[2,4*] Yeliang Wang,[1] Jia-Tao Sun,[1†] and Hong-Jun Gao[3]

1. School of Integrated Circuits and Electronics, MIIT Key Laboratory for Low-Dimensional Quantum Structure and Devices, Beijing Institute of Technology, Beijing 100081, China.

2. College of Physics and Electronic Information, Yunnan Normal University, Kunming 650500, China.

3. Beijing National Center for Condensed Matter Physics and Institute of Physics, Chinese Academy of Sciences, Beijing 100190, China

4. Yunnan Key Laboratory of Optoelectronic Information Technology, Kunming 650500, China

Abstract

Recent experiments confirm that two-dimensional (2D) boron nitride (BN) films possess room-temperature out-of-plane ferroelectricity when each BN layer is sliding with respect to each other. This ferroelectricity is attributed to the interlayered orbital hybridization or interlayer charge transfer in previous work. In this work, we attempt to understand the sliding ferroelectricity from the perspective of orbital distortion of long-pair electrons. Using the maximally localized Wannier function (MLWF) method and first-principles calculations, the out-of-plane p_z orbitals of BN are investigated. Our results indicate that the interlayer van der Waals interaction causes the distortion of the N p_z orbitals. Based on the picture of out-of-plane orbital distortion, we propose a possible mechanism to tune the ferroelectric polarization by external fields, including electric field and stress field. It is found that both the polarization intensity and direction can be modulated under the electric field. The polarization intensity of the system can also be controlled by stress field perpendicular to the plane. This study will provide theoretical help in the device design based on sliding ferroelectrics.

* Authors to whom correspondence should be addressed. Electronic addresses: fuzhm1979@163.com

† Authors to whom correspondence should be addressed. Electronic addresses: jtsun@bit.edu.cn

1. Introduction

Ferroelectric materials possessing nonvolatile and switchable spontaneous electric polarization are essential elements in diverse technology applications, including memories, field-effect transistors, solar cells, sensors, and actuators. Over the past decade, two-dimensional (2D) ferroelectric materials have attracted extensive attention due to their potential applications in the field of microelectronics. Compared with traditional ferroelectric materials, 2D ferroelectric materials are more easily integrated into functional components in miniaturized electronic devices because of their inherent nano size and ferroelectric properties [1]. In the past few years, with the large number of theoretical predictions of 2D ferroelectric materials [2-7], the intriguing ferroelectric properties of many 2D materials down to atomic thickness have been experimentally studied [8-18]. Recently, Yasuda et al. and Vizner Stern et al. showed that ferroelectricity can be engineered by artificially stacking a 2D nonpolar material such as boron nitride (BN) [19,20]. Authors attribute the sliding ferroelectricity to the interlayer orbital hybridization. Theoretical studies proposed that the ferroelectric polarization originated from net charge transfer from the upper layer to the down layer [5]. In this work, we propose the origination of sliding ferroelectricity may be understood from the orbital distortion induced by the interlayer coupling. Moreover, the tunability of the sliding ferroelectricity by external field still lack investigations in both experiments and theory, and therefore need to be addressed.

To control the ferroelectric properties of 2D materials, many strategies have been proposed, such as atomic substitution, chemical modification, supporting substrates, and application of external electric fields. For ferroelectric device, the controlling of external fields on polarization is undoubtedly more meaningful than other tuning methods. In fact, the transport, magnetism, catalysis, and other properties of 2D materials can all be modified by an external field [21-36]. A large number of relevant studies have been reported [23,33-39]. However, the external electric field effects on

the sliding ferroelectricity of 2D materials are rarely reported.

In this work, we first discuss the role of orbital distortion on the sliding ferroelectricity, and then study the ferroelectric polarization switching induced by external field application to 2D BN. We use the first-principles calculation method and the maximally localized Wannier function (MLWF) method [40] to confirm that the electric polarization comes from the distortion of the B-top N (N atom facing a B atom) $2p_z$ orbital, but the distortion of the hexagon-top N (N atom facing empty centre of the hexagon) $2p_z$ orbital also plays an important role. There is a linearly varying relationship between the polarization and electric field. Interestingly, with an increase in the electric field strength, only the distorted shape of the p_z orbital of the hexagon-top N atom greatly changes, while the distorted shape of the p_z orbital of the B-top N atom changes slightly. This is due to the different environments of the N atoms in different layers. For the N1 atom, the N $2p_z$ orbital is not only attracted by the B^{3+} ion but also repulsed by the B $2p_z$ orbital. For the N2 atom, the N $2p_z$ orbital is only subjected to the electrostatic repulsion of the p_z-orbital on the hexagon. Additionally, we find that, external pressure helps drive stronger interlayer interactions and enhances the polarization of AB (BA) stacked bilayer BN. Furthermore, the MLWF method has been used for studies of various properties of materials but rarely for studies of ferroelectricity [41-45]. This work hence bridges knowledge from different fields.

2. Computational methods

In this work, all calculations are performed using the density-functional theory (DFT) method, which is implemented in the Vienna Ab initio Simulation Package (VASP) [46-48] within the projector augmented wave (PAW) method [49]. The Perdew, Burke, and Ernzerhof (PBE) [50] parameterized generalized gradient approximation (GGA) is chosen to describe the exchange-correction functional. To accurately describe the vdW interaction in the bilayer BN systems, we adopt the empirical correction method presented by Grimme (DFT-D3) [51]. The climbing image nudged elastic band (CI-NEB) method is used to calculate the energy barriers of transition states [52].

MLWF [40,53,54] method is employed to calculate the spatial distribution of N p_z orbitals. The cut-off energy for the basis set is chosen to be 500 eV. All geometric structures are fully relaxed until the force on each atom is less than 0.02 eV/Å, and the convergence criterion is 10^{-6} eV for the electronic energy. The atomic structure is studied with a periodic slab geometry, adopting a sufficiently large vacuum layer of 15 Å to avoid interactions between adjacent layers. The optimized lattice parameter of the AB/BA stacking BN bilayer is 2.50 Å, which is in good agreement with previous values [55-57]. For geometry optimization, 9 × 9 × 1 special *k*-points are used for sampling the Brillouin zone, and denser 12 × 12 × 1 special *k*-points are set for electronic self-consistent calculations.

3. Results and discussion

3.1. Origin of ferroelectricity in AB (BA) stacked bilayer BN

Bulk *h*-BN crystals realize AA' stacking, as shown in reference [56]. This natural stacking order of a 180º-rotation restores the broken inversion symmetry in the monolayer. However, theory and experiments show that if two BN monolayers are not rotated when stacked (stacked in parallel), a polar AB or BA stacking order will be formed [56,58-60]. These configurations are parallel stacked forms with minimal local energy and are implemented as metastable crystal structures [56,58]. In AB (BA) stacking, the upper layer B (N) atom is above the lower layer N (B) atom, while the upper layer N (B) atom is above the hexagon center of the lower layer.

Let us now discuss the origin of the ferroelectric polarization. Initially, we thought that the ferroelectricity originated from hybridization between the vertically aligned B p_z orbital and N p_z orbital, which distorted the N $2p_z$ orbital. However, as seen from our calculated projected energy band structure (see figure. 1(a)) and projected density of states (see figure. 1(b)), there is no obvious hybridization between the vertically aligned B p_z orbital and N p_z orbital. Moreover, the charge transfer between the bilayer BN layers is found to be negligible by Bader charge analysis [61,62], leaving only vdW

interactions between the layers, which makes the orbital hybridization and charge transfer mechanisms invalid for the ferroelectric polarization. Previously, one of our listed authors found that the dimensional effect of SnTe ferroelectricity can be attributed to enhancement of Te p_z electron localization [63]. Thus what is the effect of N p_z electrons on the bilayer BN ferroelectricity?

As shown in figure. 1(c), (d) and (e), we calculate the N p_z orbitals of monolayer and bilayer BN using the MLWF method. According to the calculation results, the N p_z orbitals in monolayer BN are symmetric dumbbell-shaped with opposite phase signs of wannier function. However, the N p_z orbitals in bilayer AB or BA stacked BN become asymmetric or distorted. figure. 1(d) shows the unit cell of AB-stacked bilayer BN. The p_z orbitals of the two N atoms in a unit cell are distorted. The distortion of the p_z orbitals shifts the charge center upwards, creating a net dipole. Hence, the polarization direction of the AB stacking is along the negative z-axis ($-P$). The opposite case is valid for the BA stacking, whose polarization is along the positive z-axis ($+P$) (see figure. 1(e)). From the above results, the ferroelectric polarization of AB- or BA stacked bilayer BN originates from distortion of the p_z orbitals of all N atoms.

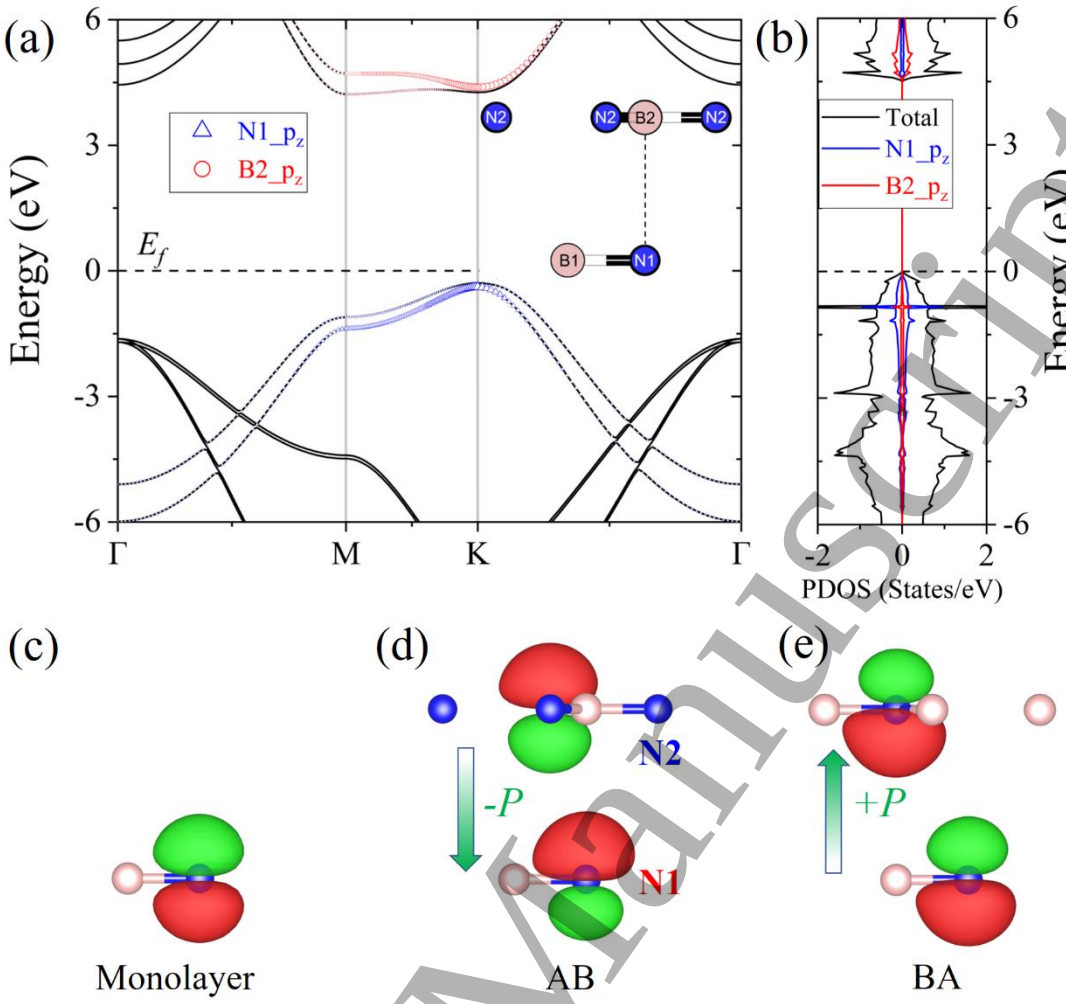

Figure. 1. The projected energy band structure (a) and projected density of states (b) of vertically aligned B atoms and N atoms as shown in the inset. The Fermi energy (E_f) is set to zero. (c), (d) and (e) represent the calculated Wannier functions of N p_z orbitals for monolayer BN, AB and BA stacking BN bilayer, where red (+) and green (-) represent the phase sign of the Wannier function.

The N atoms in different layers are in different chemical environments, which leads to different degrees of distortion of their p_z orbitals. The situation of BA stacking is completely opposite to that of AB stacking, and we will only discuss the structure of AB stacking here. In the AB stacking, the B-top N atoms (N1) lie beneath the top layer B atoms. There are both attraction and repulsion between these vertically aligned N atoms and B atoms (see figure. 2(a) and (b)). The repulsion originates from N p_z electrons and B p_z electrons (see figure. 2(a)), which can be seen according to the

momentum path interval of Γ↔M (figure. 2(d)). figure. 2(e) is the partial charge density at point ① in figure. 2(d). The red energy band corresponds to the p_z orbital of the N1 atom. The partial charge density in the Γ↔M interval on the band is similar to that in figure. 2(e), which is consistent with our model in figure. 2(a). The attraction originates from N p_z electrons and B^{3+} ions (see figure. 2(b)), which can be seen according to the band structure in the M↔K interval (figure. 2(d)).

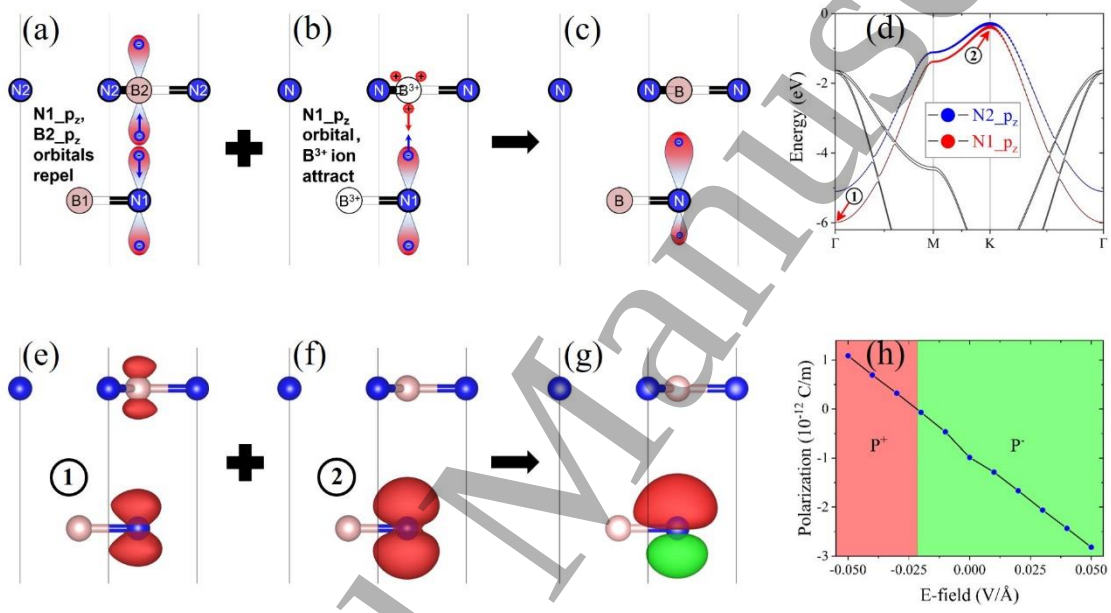

Figure. 2. (a)-(c) Schematic representation of N atom p_z orbital distortion with B and N atoms arranged vertically in a bilayer AB stacking BN. (c) Schematic diagram of N p_z orbital after distortion. (d) Projected energy band of AB stacking bilayer BN. The red and blue represents the lower layer N atom and the upper layer N atom respectively. (e) and (f) are the partial charge density at points ① and ② in figure 2(d), respectively. (g) The p_z orbital of the lower layer N atom calculated by the MLWF method. (h) Dependence of the electric polarization of bilayer AB stacking BN on the external electric field.

Figure. 2 (f) shows the partial charge density at point ② in figure. 2(d). The partial charge density in the M↔K interval on the N p_z band of the upper layer is similar to

that in figure. 2(f), which is consistent with our model in figure. 2(b). The competition between attraction and repulsion distorts the N p_z orbital of the upper layer as shown in figure. 2(c). This is consistent with the N1 p_z orbital as calculated by the MLWF method (see figure. 2(g)). The existence of these two interactions is also the reason for the stable existence of AB (BA) stacked bilayer BN. From figure. 2(d), we can conclude that the N1 p_z orbital energy is lower than that of the hexagon-top N (N2) p_z orbital. These two interactions also stabilize the distorted N1 p_z orbital. When we apply forward and reverse electric fields (the electric field is perpendicular to the 2D BN plane), the electric field preferentially modulates the shape of the N2 p_z orbital, while the shape of the N1 p_z orbital hardly changes (see figure. 3). Compared with the N1 p_z orbital, the N2 p_z orbital is only slightly distorted by the electrostatic repulsion of the p_z orbitals of B and N atoms on the facing hexagon (see figure, 1(d)). The distance between the bilayer is d = 3.43 Å. According to the charge center method, we calculate the vertical polarization of AB stacking to be -0.988×10^{-12} C/m, which is in the same order of magnitude with the Berry phase calculation of -0.805×10^{-12} C/m and previously reported value -2.08×10^{-12} C/m [5].

3.2 External electric field effects on the bilayer BN

The external electric field plays a vital role in the modulation of the electronic properties of 2D materials. In the following, we present the effect of an external uniform electric field on the electronic properties of bilayer BN for two different stacking configurations, namely, AB and BA. The electric field is applied perpendicular to the plane of the BN bilayer. The electric field strength is considered to be between 0 and 0.3 V/Å. figure 2(h) shows the relationship between the intrinsic ferroelectric polarization of AB stacked bilayer BN and the external electric field calculated by the charge centre method. When the applied electric field strength is less than -0.02 V/Å, the intrinsic ferroelectric polarization of the AB stacking is reversed. As shown in figure. 3(c), (d) and (e), the electric field tunes the polarization of AB stacked BN by adjusting the shape of the N2 p_z orbital. This also proves that the distorted N1 p_z orbital is more stable. When the electric field strength is 0.05 V/Å, the polarization strength is -2.819

$\times 10^{-12}$ C/m, and when the electric field strength is -0.05 V/Å, the polarization strength is 1.088×10^{-12} C/m. Therefore, the strength and direction of the intrinsic ferroelectric polarization of BN can be regulated by an external field.

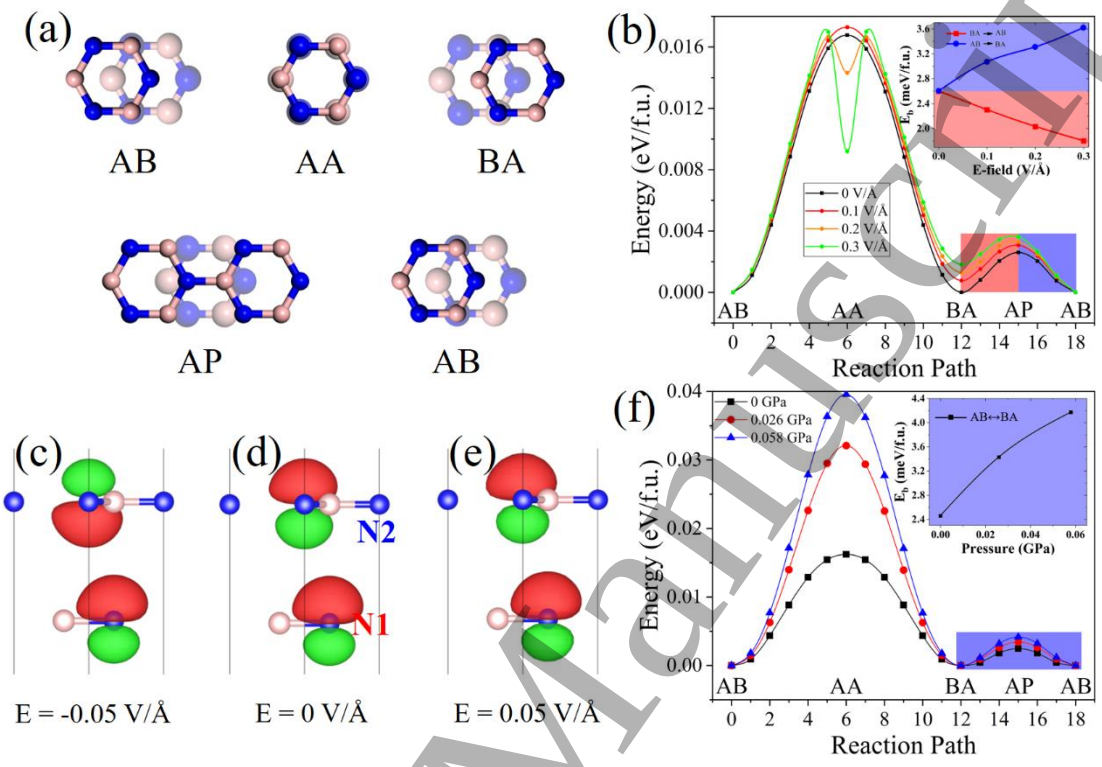

Figure. 3. Ferroelectric switching pathway of bilayer BN. (a) The top view of the structure of bilayer BN at the extreme point in figure (b) and (f). For clarity, the top (bottom) layer are represented (dimmed) by smaller (larger) atoms. (c)-(e) Variation of p_z orbital shape of N atom with applied electric field calculated by the MLWF method. The applied electric fields are -0.5 V/Å (c) and 0.5 (e) V/Å, respectively. (d) Pure AB stacked bilayer BN. (b) CI-NEB for the energy pathway for the AB ↔ BA stacked bilayer BN transformation in different applied electric fields. The inset represents the AB ↔ BA polarization switching energy barrier versus the applied electric field. (f) CI-NEB for the energy pathway for the AB ↔ BA stacked bilayer BN transformation in different applied pressure. The inset represents the AB ↔ BA polarization switching energy barrier versus the applied pressure.

From the above discussion, we know that the ferroelectric polarization

perpendicular to the bilayer BN plane can be switched by sliding one layer with respect to the other layer. The sliding pathway, *i.e.*, the ferroelectric switching pathway, is computed by using the CI-NEB method, and is shown in figure. 3(b). There are two different sliding pathways between AB and BA stacking, namely, AB→AA→BA (the AB phase slips through the AA phase to the BA phase) and AB→AP→BA (the AB phase slips through the AP phase to the BA phase). According to our calculation results, the sliding path AB→AP→BA has a low energy barrier, and the AA phase is not a stable phase in the absence of an external electric field. When the sliding energy barrier are calculated under the applied electric fields, we find that the unstable AA phase becomes stable when the electric field is 0.2 V/Å. When there is no external electric field or the external electric field is relatively small, the energy of the AA phase is at the saddle point of the energy pathway. When the external electric field strength is greater than 0.2 V/Å, the energy of the AA phase is lower than the saddle point of the energy pathway. This means that the AA, AB, and BA phases are all stable in the presence of an electric field. This result can provide theoretical help for device design. For example, in the absence of an external electric field, only two stable ferroelectric phases AB and BA can exist in the system. In this case the ferroelectric polarization (P) is switched only between $P_{\downarrow}$ and $P_{\uparrow}$. When the applied electric field strength is greater than 0.2 V/Å, there will be three stable phases, AA, AB and BA. At this time, the ferroelectric polarization will switch between P_0, $P_{\downarrow}$ and $P_{\uparrow}$.

The existence of the additional paraelectric phase AA has many possibilities in the design of logic devices. The inset of figure. 3(b) presents the switching energy barrier between the AB and BA stacking. When there is no external electric field, the sliding energy barrier between the AB and BA stacking is 2.6 meV/fu, which is close to the previous theoretical calculations [5]. When an external field exists, the sliding energy barrier from AB to BA increases, while the sliding energy barrier from BA to AB decreases. Therefore, the sliding energy barrier for AB↔BA can be regulated by the external field.

3.3 Pressure effects on the bilayer BN

Altering the electronic structure and interlayer distance by applying high pressure is a promising strategy to tune the interlayer coupling, which is a well-established approach for tuning physical properties, but it is rarely used in the study of ultrathin quantum systems. High pressure has been shown in the past few years to be a powerful tool to change the electronic structure of materials and even promote the phase transition of materials [64,65]. The effect of pressure on the ferroelectric properties of BN was calculated by changing the interlayer spacing and fixing the *z*-axis coordinates of the atoms. When the pressure is 0.026 GPa, the ferroelectric polarization of AB stacked bilayer BN is -1.161×10^{-12} C/m, and when the pressure is 0.058 GPa, the ferroelectric polarization is -1.364×10^{-12} C/m. Therefore, the ferroelectric polarization strength of BN can be enhanced by pressure. We also use the MLWF method to calculate the shape of the p_z orbital of the N atom under different pressures. The calculation results show that pressure has little effect on the distortion of the p_z orbital of the N atom. The inset in figure. 3(f) shows the ferroelectric switching energy barrier versus pressure. The ferroelectric sliding barrier increases with increasing pressure. According to the above conclusions, pressure can not only enhance the ferroelectric polarization of BN but also stabilize its polarization.

4. Conclusions

In summary, for 2D AB or BA stacked bilayer BN, we studied the effects of an external electric field and pressure on ferroelectricity, and the possible origin of the out-of-plane ferroelectric polarization. Both the external electric field and pressure can significantly enhance the ferroelectric polarization of BN. In particular, the electric field can flip the polarization direction of BN. There are both repulsive and attractive interactions between vertically aligned N atoms and B atoms. The former originates from N p_z electrons and B p_z electrons. The latter originates from N p_z electrons and B^{3+} ions. These two interactions lead to distortion of the B-top N p_z orbital. The hexagon-top N p_z orbital is also distorted by the electrostatic repulsion of the p_z orbitals of B and N atoms on the facing hexagon. These two N p_z orbital distortions collectively determine the strength of the ferroelectric polarization. When the electric field is

sufficiently large, the paraelectric phase AA becomes stable, which may help the design of logic devices.

Acknowledgements

This work was supported by National Key Research and Development Program of China (Grants Nos. 2020YFA0308800), "Strategic Priority Research Program (B)" of Chinese Academy of Sciences (Grant No. XDB30000000), National Natural Science Foundation of China (Grant No. 11974045, 12264055). The computational resources were provided by the Shanghai Supercomputing Center.

References

[1] M. Wu and P. Jena, WIREs Comput. Mol. Sci. **8**, e1365 (2018).
[2] E. Bruyer, D. Di Sante, P. Barone, A. Stroppa, M.-H. Whangbo, and S. Picozzi, Phys. Rev. B **94**, 195402 (2016).
[3] D. Di Sante, A. Stroppa, P. Barone, M.-H. Whangbo, and S. Picozzi, Phys. Rev. B **91**, 161401 (2015).
[4] W. Ding, J. Zhu, Z. Wang, Y. Gao, D. Xiao, Y. Gu, Z. Zhang, and W. Zhu, Nat. Commun. **8**, 14956 (2017).
[5] L. Li and M. Wu, ACS Nano **11**, 6382 (2017).
[6] M. Wu and X. C. Zeng, Nano Lett **16**, 3236 (2016).
[7] M. Wu and X. C. Zeng, Nano Lett **17**, 6309 (2017).
[8] S. N. Shirodkar and U. V. Waghmare, Phys. Rev. Lett. **112**, 157601 (2014).
[9] S. Wan, Y. Li, W. Li, X. Mao, W. Zhu, and H. Zeng, Nanoscale **10**, 14885 (2018).
[10] A. Belianinov, Q. He, A. Dziaugys, P. Maksymovych, E. Eliseev, A. Borisevich, A. Morozovska, J. Banys, Y. Vysochanskii, and S. V. Kalinin, Nano Lett **15**, 3808 (2015).
[11] M. Chyasnavichyus, M. A. Susner, A. V. Ievlev, E. A. Eliseev, S. V. Kalinin, N. Balke, A. N. Morozovska, M. A. McGuire, and P. Maksymovych, Appl. Phys. Lett. **109**, 172901 (2016).
[12] B. Xu, H. Xiang, Y. Xia, K. Jiang, X. Wan, J. He, J. Yin, and Z. Liu, Nanoscale **9**, 8427 (2017).
[13] W. Song, R. Fei, and L. Yang, Phys. Rev. B **96**, 235420 (2017).
[14] S. A. Tawfik, J. R. Reimers, C. Stampfl, and M. J. Ford, J. Phys. Chem. C **122**, 22675 (2018).
[15] C. Xiao, F. Wang, S. A. Yang, Y. Lu, Y. Feng, and S. Zhang, Adv. Funct. Mater. **28**, 1707383 (2018).
[16] K. Chang *et al.*, Science **353**, 274 (2016).

[17] Y. Bao *et al.*, Nano Lett **19**, 5109 (2019).
[18] C. R. Woods, P. Ares, H. Nevison-Andrews, M. J. Holwill, R. Fabregas, F. Guinea, A. K. Geim, K. S. Novoselov, N. R. Walet, and L. Fumagalli, Nat. Commun. **12**, 347 (2021).
[19] K. Yasuda, X. Wang, K. Watanabe, T. Taniguchi, and P. Jarillo-Herrero, Science **372**, 1458 (2021).
[20] M. Vizner Stern, Y. Waschitz, W. Cao, I. Nevo, K. Watanabe, T. Taniguchi, E. Sela, M. Urbakh, O. Hod, and M. Ben Shalom, Science **372**, 1462 (2021).
[21] X. Jiang *et al.*, Nat. Commun. **13**, 574 (2022).
[22] A. Bafekry, M. M. Obeid, C. V. Nguyen, M. Ghergherehchi, and M. Bagheri Tagani, J. Mater. Chem. A **8**, 13248 (2020).
[23] A. Bafekry and M. Neek-Amal, Phys. Rev. B **101**, 085417 (2020).
[24] M. M. Obeid, Appl. Surf. Sci. **508**, 144824 (2020).
[25] A. Bafekry, Phys. E. **118**, 113850 (2020).
[26] A. Bafekry, C. Stampfl, B. Akgenc, B. Mortazavi, M. Ghergherehchi, and C. V. Nguyen, Phys. Chem. Chem. Phys. **22**, 6418 (2020).
[27] C. V. Nguyen and N. N. Hieu, Chem. Phys. **468**, 9 (2016).
[28] A. Bafekry, C. Stampfl, and F. M. Peeters, Sci. Rep. **10**, 213 (2020).
[29] K. D. Pham *et al.*, Chem. Phys. Lett. **716**, 155 (2019).
[30] A. Bafekry, M. Ghergherehchi, and S. Farjami Shayesteh, Phys. Chem. Chem. Phys. **21**, 10552 (2019).
[31] T. V. Vu, N. V. Hieu, L. T. P. Thao, N. N. Hieu, H. V. Phuc, H. D. Bui, M. Idrees, B. Amin, L. M. Duc, and C. V. Nguyen, Phys. Chem. Chem. Phys. **21**, 22140 (2019).
[32] S. Yin, Q. Luo, D. Wei, G. Guo, X. Sun, Y. Li, Y. Tang, Z. Feng, and X. Dai, Phys. E. **142**, 115258 (2022).
[33] Z. Chang, K. Yuan, Z. Sun, X. Zhang, Y. Gao, G. Qin, and D. Tang, Phys. Chem. Chem. Phys. **23**, 13633 (2021).
[34] P. Kumar, B. S. Bhadoria, S. Kumar, S. Bhowmick, Y. S. Chauhan, and A. Agarwal, Phys. Rev. B **93**, 195428 (2016).
[35] E. J. G. Santos and E. Kaxiras, Nano Lett **13**, 898 (2013).
[36] F. Ahmed, Y. D. Kim, M. S. Choi, X. Liu, D. Qu, Z. Yang, J. Hu, I. P. Herman, J. Hone, and W. J. Yoo, Adv. Funct. Mater. **27**, 1604025 (2017).
[37] G. Groetzinger, Nature **135**, 1001 (1935).
[38] W. H. Huber, L. M. Hernandez, and A. M. Goldman, Phys. Rev. B **62**, 8588 (2000).
[39] V. E. Dorgan, A. Behnam, H. J. Conley, K. I. Bolotin, and E. Pop, Nano Lett **13**, 4581 (2013).
[40] A. A. Mostofi, J. R. Yates, Y.-S. Lee, I. Souza, D. Vanderbilt, and N. Marzari, Comput. Phys. Commun. **178**, 685 (2008).
[41] N. Marzari, A. A. Mostofi, J. R. Yates, I. Souza, and D. Vanderbilt, Rev. Mod. Phys. **84**, 1419 (2012).
[42] J. Qiao, J. Zhou, Z. Yuan, and W. Zhao, Phys. Rev. B **98**, 214402 (2018).
[43] M. C. Romano, A. Vellasco-Gomes, and A. Bruno-Alfonso, J. Opt. Soc. Am. B

35, 826 (2018).
[44] J. H. Ryoo, C.-H. Park, and I. Souza, Phys. Rev. B **99**, 235113 (2019).
[45] Z. Fu, B. Yang, and R. Wu, Phys. Rev. Lett. **125**, 156001 (2020).
[46] G. Kresse and J. Hafner, Phys. Rev. B **47**, 558 (1993).
[47] G. Kresse and J. Furthmüller, Phys. Rev. B **54**, 11169 (1996).
[48] J. Hafner, J. Comput. Chem. **29**, 2044 (2008).
[49] P. E. Blöchl, Phys. Rev. B **50**, 17953 (1994).
[50] J. P. Perdew, K. Burke, and M. Ernzerhof, Phys. Rev. Lett. **80**, 891 (1998).
[51] X. Wu, M. C. Vargas, S. Nayak, V. Lotrich, and G. Scoles, J. Chem. Phys. **115**, 8748 (2001).
[52] G. Henkelman, B. P. Uberuaga, and H. Jónsson, J. Chem. Phys. **113**, 9901 (2000).
[53] N. Marzari and D. Vanderbilt, Phys. Rev. B **56**, 12847 (1997).
[54] I. Souza, N. Marzari, and D. Vanderbilt, Phys. Rev. B **65**, 035109 (2001).
[55] R. M. Ribeiro and N. M. R. Peres, Phys. Rev. B **83**, 235312 (2011).
[56] G. Constantinescu, A. Kuc, and T. Heine, Phys. Rev. Lett. **111**, 036104 (2013).
[57] R. S. Pease, Nature **165**, 722 (1950).
[58] S. Zhou, J. Han, S. Dai, J. Sun, and D. J. Srolovitz, Phys. Rev. B **92**, 155438 (2015).
[59] J. H. Warner, M. H. Rümmeli, A. Bachmatiuk, and B. Büchner, ACS Nano **4**, 1299 (2010).
[60] C.-J. Kim, L. Brown, M. W. Graham, R. Hovden, R. W. Havener, P. L. McEuen, D. A. Muller, and J. Park, Nano Lett **13**, 5660 (2013).
[61] W. Tang, E. Sanville, and G. Henkelman, J. Phys.: Condens. Matter **21**, 084204 (2009).
[62] R. F. J. C. R. Bader, Chem. Rev. **91**, 893 (1991).
[63] Z. Fu, M. Liu, and Z. Yang, Phys. Rev. B **99**, 205425 (2019).
[64] Z.-H. Chi, X.-M. Zhao, H. Zhang, A. F. Goncharov, S. S. Lobanov, T. Kagayama, M. Sakata, and X.-J. Chen, Phys. Rev. Lett. **113**, 036802 (2014).
[65] L. Fu *et al.*, Sci. Adv. **3**, e1700162 (2017).